ELSEVIER

Journal of Hydrology 267 (2002) 173–185

Journal of Hydrology

www.elsevier.com/locate/jhydrol

Variations of self-potential and unsaturated water flow with time in sandy loam and clay loam soils

Claude Doussan[a,*], Laurence Jouniaux[b], Jean-Louis Thony[c]

[a]*INRA, Unité Climat, Sol & Environnement, Domaine Saint Paul, Site Agroparc, 84914 Avignon Cedex 9, France*
[b]*Ecole Normale Supérieure, Laboratoire de Géologie, UMR 8538, 24, rue Lhomond, 75231 Paris Cedex 05, France*
[c]*Laboratoire d'étude des Transferts en Hydrologie et Environnement, BP53-F-38041 Grenoble Cedex 09, France*

Abstract

Accurate assessment of soil–water fluxes is essential in soil physics due to its direct implications in environmental, agronomical or hydrological applications. Field estimations of soil–water fluxes by 'classical' hydraulic methods are often difficult to obtain. Moreover, water fluxes are highly variable in space and time. The obtainment of a reasonable estimate for this variable would require numerous measurement sites. However, such a requirement is rarely met. Thony et al. [CR Acad. Sci. Paris, Earth Planetary Sci. 325 (1997) 317] presented the experimental evidence of a linear relationship between the self-potential (SP) and the unsaturated soil–water flux. Therefore, this relationship would allow the indirect assessment of the water flux using electrical measurements. Such an approach would appear much more flexible and easier to perform than the current hydraulic measurements. The aim of this study is to experimentally investigate the existence and robustness of the flux–SP relationship for different soil types and pedoclimatic conditions.

The soil–water fluxes and the SP were monitored in a long-term experiment involving two types of soils, contrasting in hydraulic and electric properties. The soils were placed in lysimeters which were instrumented with tensiometers and TDR probes for monitoring hydraulic heads and moisture content, respectively. Unpolarizable SP electrodes, temperature sensors and suction cups (for collecting pore water) were also installed in the lysimeters. The SP and the fluxes were measured or calculated in the 30–40 cm depth section.

Results show that the variations of the SP with time were clearly linked to both rainfall events and evaporation. However, in the long-term, the linear relationship between the unsaturated water flux and the SP evolves from strongly correlated to almost not correlated. The slope (sensitivity) of the flux–SP relationship varies with the soil type, decreasing with more electrically conductive soil. Taking into account a varying soil–electrode contact greatly improves the flux–SP relationship at the scale of the rainfall event, particularly when considering infiltration and drainage phases separately. Nevertheless, at the scale of a year, with alternated rainfalls and evaporation phases, the robustness of the relationship decreases (i.e. the coefficients of the relationship vary between events). This variability could be related to time variations in electrical conductivity, not so much to that of the soil–water, but rather to that of the water from the salted soil mud added to the SP electrodes at the time of installation.

This study points out methodological problems associated with the measurement of SP in shallow unsaturated soils over the long-term and the need for designing specific electrodes for this purpose. However, in deep soils beneath the root zone, environmental conditions generally vary slowly and lightly in comparison to surface horizons. In this case and with our present set of SP measurement devices, the flux–SP relationship could be more stable than in the surface soil horizons and useful for examining aquifer recharge, capillary rises or contaminant transfer.

Keywords: Unsaturated flow; Self-potential; Soil; Fluxmeter

* Corresponding author. Fax: +33-4-3272-2238.
E-mail address: doussan@avignon.inra.fr (C. Doussan).

0022-1694/02/$ - see front matter
PII: S0022-1694(02)00148-8

1. Introduction

The fact that the water flow in a porous medium induces electric fields has been known for a long time (Ahmad, 1964). Such evidence has been observed in different geologic settings such as volcanoes, tectonically active areas, in the vicinity of dams or lakes, or in quarries (Mitzutani et al., 1976; Ishido, 1989; Morat and Le Mouël, 1992; Aubert and Dana, 1994; Hashimoto and Tanaka, 1995; Perrier et al., 1998). However, a quantitative relationship between the flow and the electric field is most often assumed rather than observed because simultaneous detailed measurements of the electric and hydraulic parameters are seldom available.

The self-potential (SP) is generated by the existence of a natural gradient of electric potential. In field situations, SP may arise: (i) from a thermoelectric potential, consequence of a temperature gradient, (ii) from a chemical potential, consequence of chemical gradients, and (iii) from a streaming potential, electrokinetic phenomena, consequence of fluid pressure gradients. SP anomalies are often assumed to result primarily from electrokinetic phenomena because the thermoelectric and chemical coefficients are smaller than the electrokinetic coefficient (Perrier et al., 1999; Jouniaux et al., 2000).

In a saturated porous medium, the differential motion between the fluid and the solid induces electrokinetic phenomena. Minerals forming the porous medium, which are usually negatively charged, create an electric double layer in the pore fluid. A strong electric field is created perpendicular to the surface of the mineral, which attracts cations and repulses anions in the vicinity of the solid–liquid interface. The electric double layer is made up of: (i) the Stern layer, which includes the hydration of the virgin surface as well as ions weakly bound to the surface, and (ii) the Gouy diffuse layer, where Coulomb forces are counterbalanced by thermal agitation (for detailed description see Adamson (1976), Dukhin and Derjaguin (1974) and Hunter (1981)). The streaming potential is due to the motion of the diffuse layer along with fluid flow, induced by a pressure gradient. The shear plane in the fluid, i.e. the zero velocity surface, is located within the diffuse layer. The electric potential along this surface is called the zeta potential.

Fluids moving through porous media or capillaries generate streaming potentials that are governed by the Helmholtz–Smoluchowski equation as discussed below (Overbeek, 1952; Nourbehecht, 1963).

In a saturated porous medium the electric current density I (A/m^2) and the fluid flow J (m/s) are coupled according to the following equations:

$$-I = \frac{\sigma_f}{F}\,\mathrm{grad}\,V - \frac{\varepsilon\zeta}{\eta F^0}\,\mathrm{grad}\,P \tag{1}$$

$$-J = -\frac{\varepsilon\zeta}{\eta F^0}\,\mathrm{grad}\,V + \frac{k}{\eta}\,\mathrm{grad}\,P \tag{2}$$

where V is the electric potential, P the fluid pressure, σ_f and ε the electrical conductivity and the dielectric constant of the fluid, respectively, ζ the zeta potential, η the dynamic viscosity of the fluid and k is the permeability of the porous medium. F^0 is the formation factor, i.e. the ratio between fluid and rock electrical conductivity ($\sigma_{fluid}/\sigma_{rock}$) for a high fluid conductivity when electrical surface conductivity is negligible, and F is the formation factor for the fluid conductivity being studied (i.e. possibly with electrical surface conductivity). The first term on the right-hand side in Eq. (1) is Ohm's law, and the second term in Eq. (2) is Darcy's law. At steady state, the convection current (related to grad P—Eq. (1)) is balanced by the conduction current (related to grad V—Eq. (1)). Equating these currents leads to the ratio $\Delta V/\Delta P$, called the streaming-potential cross-coupling coefficient C_s, or simply, the coupling coefficient according to Eq. (3):

$$C_s = \frac{\Delta V}{\Delta P} = \frac{\varepsilon\zeta}{\eta\sigma_f}\frac{F}{F^0} \tag{3}$$

which is the Helmholtz–Smoluchowski equation (Dukhin and Derjaguin, 1974). ΔV is the generated electric potential difference and ΔP is the pore-pressure difference, between two points in the porous medium. The above equations are recalled here because they are found in different forms in the literature (Ishido and Mizutani, 1981; Pride, 1994). For a complete development of the equations governing the coupled electromagnetics and flow through porous media, see Pride (1994) and Revil (1999a,b). Eq. (3) implies that the currents are of equal magnitude and opposite along the same path. When the surface conductivity is negligible, $F = F^0$, and

Eq. (3) can be written as:

$$C_s = \frac{\Delta V}{\Delta P} = \frac{\varepsilon\zeta}{\eta\sigma_f} \quad (4)$$

Eq. (3) or (4) can be rewritten in terms of fluid flow, taking into account Darcy's law for a saturated porous medium:

$$F = \frac{K}{C_s}\Delta V \quad (5)$$

where F is the (Darcy) flux of water and K is the saturated hydraulic conductivity. When interpreting the SP data as the result of an electrokinetic process, Eq. (5) shows that a linear relationship is also expected between the water flux and the SP for a saturated porous medium.

The linear relationships represented in Eq. (4) or (5) between the pressure gradient or the water flux and the electric potential have been observed and validated for different unconsolidated or consolidated sediments and rocks (Ahmad, 1964; Jouniaux and Pozzi, 1995; Lorne et al., 1999; Jouniaux et al., 2000). However, very few measurements of the SP for conditions of *unsaturated* fluid flow are available, particularly for soils. The field experiments of Thony et al. (1997), where the soil–water fluxes and the electric potentials were measured independently during a rainfall event, brought evidences of the existence of a linear relationship between the unsaturated water flux in soil and the SP.

Estimation of soil–water fluxes is essential in soil physics due to its direct implications in environmental, agronomical or hydrological purposes (i.e. estimation of drainage, evaporation, transfer of pollutants, aquifer recharge, infiltration/runoff partition, etc.). Field estimation of soil–water fluxes is usually done either by mass balance, such as the 'zero flux method' (Vachaud et al., 1978), or by direct application of the Darcy's law extended for unsaturated flow. The latter requires an initial determination of the soil hydrodynamic characteristics (water retention, unsaturated hydraulic conductivity) as a function of water potential (or soil moisture) on soil core samples in the laboratory (Tamari et al., 1993). However, these widely used hydraulic methods present some difficulties. They are rather difficult to set-up and manage, time consuming, they require specific equipment (for measuring the soil moisture and water potential) and problems can be encountered during the data interpretation process. Moreover, water fluxes (as well as hydraulic conductivity or soil moisture) are highly variable in time and space and an accurate determination of these properties at different scales would require a high number of measuring sites. These requirements are rarely met due to the time needed and the complexity of the measurements. Therefore, new ways and devices for estimating soil–water fluxes would be very helpful, such as an 'unsaturated fluxmeter'. Gee et al. (1999) presented a design using a heat pulse, but the estimation of the flux is not straightforward. Based on the fact that SP measurements could be easier to perform than the hydraulic methods and based on the possible linearity of the SP–flux relationship, this study aims at estimating soil–water fluxes from SP measurements in soils. Therefore, questions have to be answered regarding: (i) the stability of such a relationship, in different soil types and pedoclimatic conditions, (ii) its robustness with time and the sensitivity of the signal, and (iii) the influence of environmental factors on the relationship.

This article attempts to experimentally address these questions, and more specifically the stability and reproducibility of the relationship between the SP and the unsaturated soil–water fluxes, at a space scale intermediate between the laboratory column and the field, i.e. the scale of a few square meters in lysimeters.

2. Materials and methods

2.1. Experimental sites

The experimental sites consist of two non-weighting lysimeters each of about 9 m^2 surface area and 2 m depth, located in the south of France (Avignon, lat.: 43°55′00″N, long.: 4°52′47″E) in the INRA experimental fields (Fig. 1). One lysimeter is packed with a sandy loam soil and the other with a clay loam soil. The soils were kept bare during the experiment. The climate of the region is Mediterranean and shows a large inter annual variability.

2.2. Instrumentation

Hydraulic heads were measured with automatic

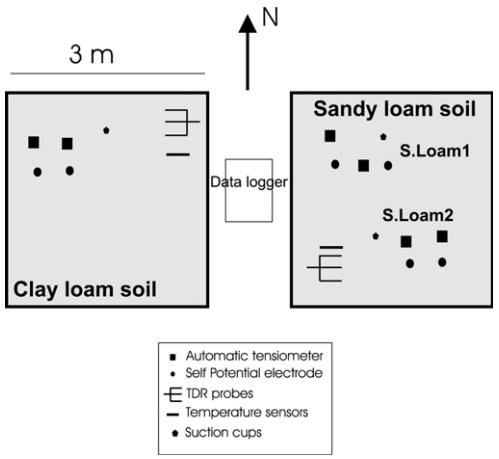

Fig. 1. Schematic map of the experimental sites (two lysimeters filled with clay loam or sandy loam) including probes locations. S. Loam 1 and S. Loam 2 are the two measuring points in the sandy loam.

tensiometers (SDEC, France) at two depths: 30 and 40 cm. SP measurements were performed with unpolarizable electrodes ($Pb/PbCl_2$ type, Petiau, 2000; SDEC-France) at identical depths installed at about 20 cm from the tensiometers. These electrodes were selected for their long-term stability and low noise characteristics (Perrier et al., 1997; Petiau, 2000). The electrodes were vertically installed in the soil. Soil from the site, which was mixed with NaCl saturated water to form mud, was added at the bottom of the holes in which the SP electrodes were inserted. Adding this mud allowed us to get identical geochemical conditions near all the electrodes and a good soil–electrode contact. Moisture content was measured with a set of TDR probes (Time Domain Reflectometry, Trase system) implanted at 5, 15, 30 and 40 cm depths. Soil temperature was also monitored at these depths with Pt-thermistances. Temperature, SP and hydraulic heads measurements were recorded with a data logger (CR10X, Campbell) of high input impedance. Two data acquisition locations (i.e. a pair of electrodes and tensiometers) were chosen in the sandy loam lysimeter (herein called S. Loam 1 and S. Loam 2) and one in the clay loam lysimeter. Electrodes in the sandy loam were referenced to the same electrode buried at 40 cm. The SP was measured as $V_{40cm} - V_{30cm}$, where V is the electric potential at the indicated depth. Suction cups were also installed at 35 cm depth in order to sample the soil pore water and to determine the electrical conductivity of the solution. Two suctions cups were installed in the same way as the electrodes, i.e. with salted soil mud, to estimate time variations of the electrical conductivity of the mud pore water.

2.3. Water flux determination and SP correction

Mean water flux at 35 cm depth was calculated by Darcy's law using hydraulic heads measured at 30 and 40 cm depth. The hydraulic conductivity was calculated for the mean matric potential of the 30–40 cm depth section. Unsaturated hydraulic conductivity (which depends on the moisture content or matric potential in unsaturated flow—Hillel, 1974) and water retention (i.e. relationship between moisture content and matric potential) were determined in the laboratory using the Wind evaporation method (Tamari et al., 1993) on soil cores sampled at the end of the experiment. Fig. 2 presents these hydrodynamic characteristics of the sandy loam.

The SP was corrected for temperature variations at 35 cm depth using the sensitivity coefficient of these electrodes, that is 0.21 mV/°C (Petiau, 2000).

3. Results

Water potential variations. Time variations of total water potential over a 6 month period are shown in Fig. 3. After a rainy autumn in 1999 that refilled the soil with water after the summer, the winter 2000 was a very dry season with almost no rain. Potential evapotranspiration (~ 2 mm d^{-1}, data not shown) was rather low, but sufficient to induce evaporation during this period. This explains why the water potential dropped from about -1.5 m to between -5 and -6 m in the sandy loam. In the clay loam, the fall of the water potential was much steeper, from -4 m to less than -8 m in February, unfortunately below the working range of tensiometers. In the early spring 2000, a series of rainfalls occurred more or less regularly. This induced a quick rise of the water potential in the sandy loam, which reacted rapidly to the rain at 30–40 cm depth. The water potential in the clay loam recovered much more slowly during this rainy period. In the late spring/beginning of summer, the water potential of both soil types sharply declined

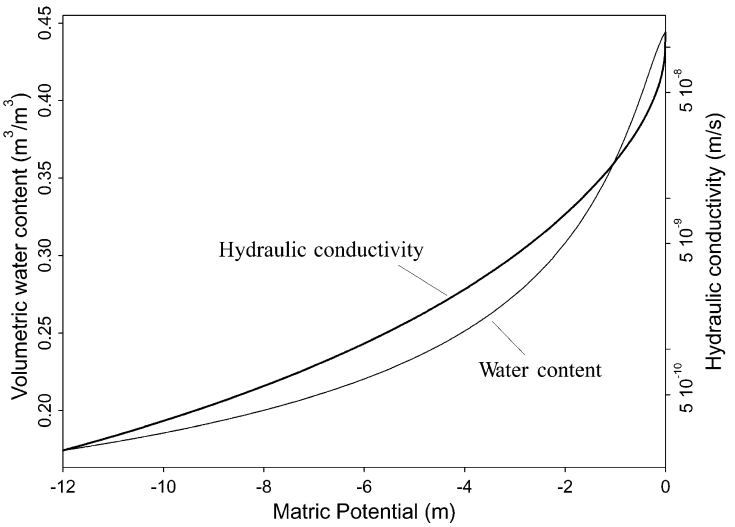

Fig. 2. Hydrodynamic characteristics (water retention and hydraulic conductivity) of the sandy loam soil used in the experiments as a function of matric potential.

because of the increase in potential evapotranspiration ($\sim$5.5–6 mm d^{-1}). As a consequence, the tensiometers were brought out of the working range. It should be noted that, in the case of the sandy loam soil, although the overall tendency is similar for the two measurement points (S. Loam 1 and S. Loam 2), the amplitude of variation differs, showing some heterogeneity in the hydraulic behaviour of the soil.

3.1. Self-potential variations

Self-potential variations, i.e. $V_{40cm} - V_{30cm}$: the

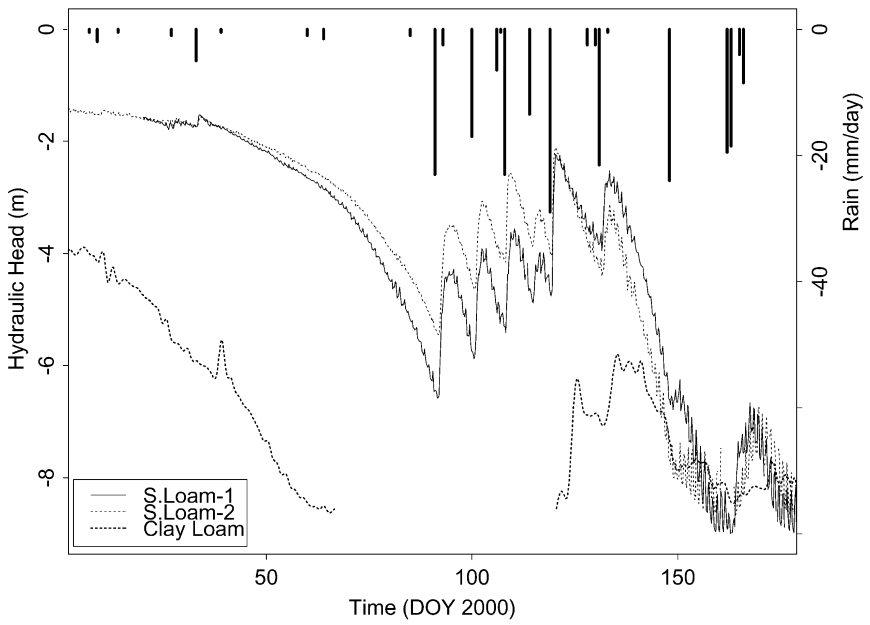

Fig. 3. Time variation of the mean hydraulic head (or total water potential) at 35 cm depth for the two measuring points (S. Loam 1 and S. Loam 2) in the sandy loam lysimeter, and in the clay loam lysimeter. Daily rainfall is also presented (vertical lines).

electric potential difference between 40 and 30 cm depth, are presented in Fig. 4 for the two types of soil. The amplitude of variation for the sandy loam was about 60 mV over the year and 40 mV between January and June. In the clay loam, variations are less pronounced with a yearly amplitude of about 20 mV. The electric field at 35 cm depth (approximated by $(V_{40cm} - V_{30cm})/\Delta z$ with$\Delta z = 10$ cm) ranges between -150 mV/m and $+400$ mV/m in the sandy loam and between -150 mV/m and $+40$ mV/m in the clay loam. These variations are much higher than those found by Thony et al. (1997), which ranged between -1 and $+35$ mV/m during a single rainfall event. Diurnal variations of about 1 mV are also noticeable in the sandy loam, whereas in the clay loam the electric signal appears much less noisy. When comparing the electric data at the two measuring points in the sandy loam, the pattern of variation looks similar but the different amplitudes of the signals denotes some heterogeneity in the lysimeter, as it was the case for water. The high rates of variation of the SP observed in the sandy loam are most often linked to rainfall events that started at the beginning of spring (day 91, Fig. 4). The events resulted in a delayed peak in the SP data. The SP measurements are here interpreted as electrokinetic processes, so that the measured electric field is induced by infiltration of water in soil and the high pressure gradient associated (see Eq. (4)). The zeta potential and the water electrical conductivity are expected to be constant or slightly varying for a given soil type (see Section 3.3). However, some variations of the SP seem unrelated to rainfalls, e.g. in winter (around day 20). In the clay loam, time variations are generally much smoother but also show some jumps (e.g. around day 60 and 130) with no clear relation to rainfall events. In particular, the strong variation around day 60 happened in the dry winter period (see rains in Fig. 4).

3.2. Unsaturated water flux

Time variations of mean water fluxes at 35 cm depth, calculated from the observed water potential gradients and from the calculated hydraulic conductivity, are presented in Fig. 5. For the sandy loam, the calculated water flux at the beginning of the period appears to be noisy because the hydraulic gradients are very small. This indicates that water in the soil is near hydrostatic equilibrium and a small error in pressure measurements induces a large variation of low fluxes. A clear upward water flux (evaporation) started around day 50 (February) and levelled off on day 91 (end of March), when rain started. From that moment on, fluxes were directed downward (infiltration), with more or less pronounced peaks appearing slightly after the rainfall events. The base line of infiltration went back to zero (null flux) at the end of spring. The differences between the two measurement points of the sandy loam are clearly seen in Fig. 5, where the infiltration rates are greater than 0.6 cm d^{-1} in S. Loam 1, whereas they do not exceed 0.2 cm d^{-1} in S. Loam 2.

In the clay loam, less flux data are available because tensiometers were at the limit of, or out of the working range part of the time. However, fluxes are much smaller than in the sandy loam and the water dynamics look completely different showing, in particular, higher fluxes at the beginning of the year 2000.

3.3. Unsaturated flux–self-potential relationship

The SP and the unsaturated water fluxes appear to be related to each other (Figs. 4 and 5). They show the same global trends and peaks. However, it is shown in Fig. 6 and in Table 1 that a simple linear correlation between the fluxes and the SP (i.e. Flux $= a$SP $+ b$) is relatively weak for the whole period including evaporation and infiltration, between days 30 and 140. The slope of the flux–SP relationship seems to be much higher in the sandy loam than in the clay loam, probably because the clay loam electrical conductivity is greater than that of the sandy loam. In the rest of the discussion the focus will be set more specifically on the sandy loam because more data are available, but the results and conclusions are qualitatively the same for both soil types.

When looking at the scale of a single rainfall event, contrasted results are obtained concerning the flux–SP relationship. For example, Fig. 7 and Table 1 present data for the first rainfall in the spring for the sandy loam soil. A strong linear correlation is observed between the fluxes and the SP for the S. Loam 1 point. This correlation is greatly increased when the fluxes and the SP are daily averaged, as in

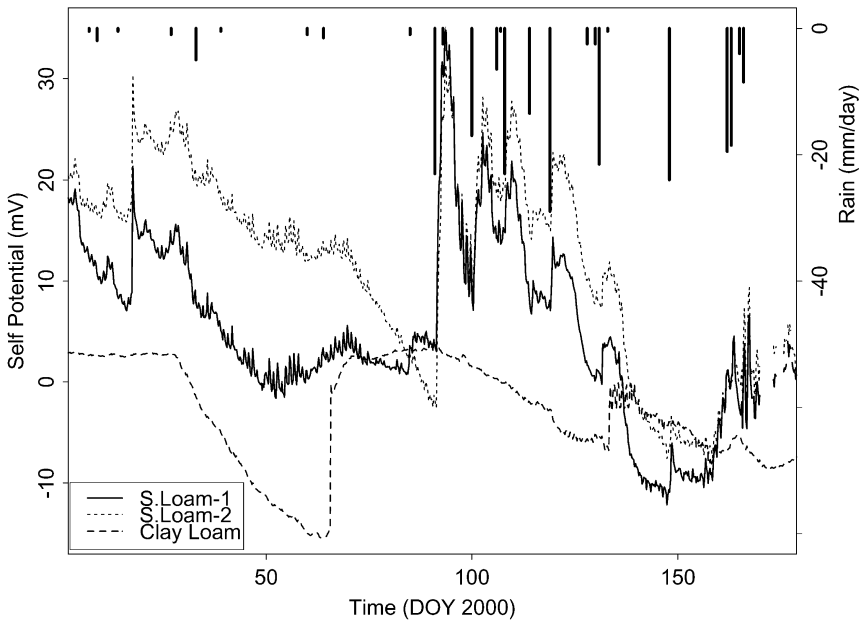

Fig. 4. Time variation of the self-potential between 30 and 40 cm depths (i.e. $V_{40cm} - V_{30cm}$, where V is the electric potential at indicated depth) for the two measuring points (S. Loam 1 and S. Loam 2) in the sandy loam lysimeter, and in the clay loam lysimeter. Daily rainfall is also presented (vertical lines).

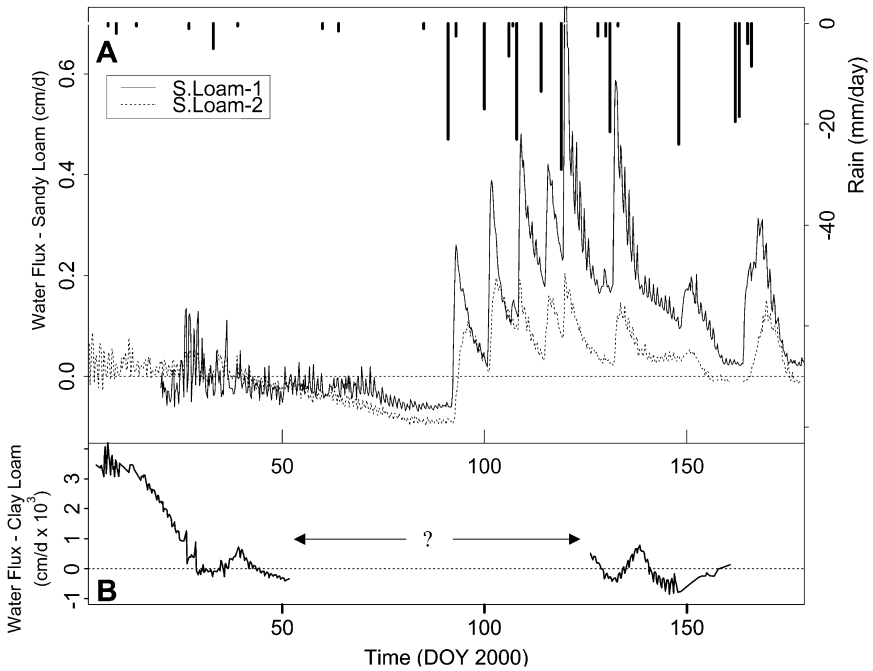

Fig. 5. Calculated soil–water fluxes (from the hydraulic conductivity and hydraulic heads data) at 35 cm depth for the two measuring points (S. Loam 1 and S. Loam 2) in the sandy loam lysimeter (A) and in the clay loam lysimeter (B). The '?' mark signifies that hydraulic heads could not be measured at that time and therefore water flux is not available. Daily rainfall is also presented (vertical lines).

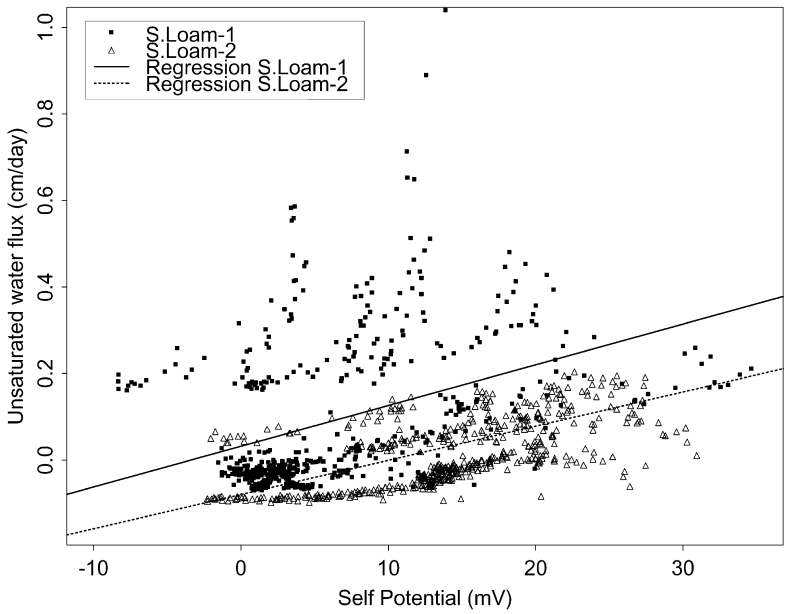

Fig. 6. Relationship between SP at 30 and 40 cm depth (i.e. $V_{40cm} - V_{30cm}$, where V is the electric potential at indicated depth) and the soil–water flux at 35 cm depth for the two measuring points (S. Loam 1 and S. Loam 2) in the sandy loam lysimeter for the period 30–140 day of year 2000, encompassing evaporation and infiltration phases. Regression lines Flux $= a\mathrm{SP} + b$ are also shown (see Table 1 also).

Thony et al. (1997) experiment, reaching nearly the same correlation level ($r^2 = 0.912$) in the two experiments. Nevertheless, this correlation vanishes for the S. Loam 2 point (Fig. 7).

Some processes altering the SP signal and consequently the flux–SP relationship may explain such variations. When examining the SP records (Fig. 4), abrupt variations of SP are observed that are not related to infiltration (e.g. around day 20 in the sandy loam and day 65 in the clay loam). This suggests that some miscontact between the soil and the electrode may have occurred in this long-term experiment. Miscontact may be directly due to variations in the soil–water saturation near the electrodes, or variations in the electrode porous material that separates the (gel) electrolyte from the soil. It may also be indirectly related to swelling and shrinkage of the soil that leads to cracks at the soil–electrode interface. If we use the water saturation to take into account the effects of varying soil–electrode contact (as in some plant root water uptake models for simulating the soil–root contact, Jensen et al., 1993), the relationship between the fluxes and the SP can be

Table 1
Coefficients of the linear regression between SP (i.e. $V_{40cm} - V_{30cm}$, where V is the electric potential at indicated depth) and soil–water flux at 35 cm depth (Flux $= a\mathrm{SP} + b$) for a 3 month period (for the two measuring points of the sandy loam lysimeter and for the clay loam lysimeter) and for the first rainfall event (23 mm) in spring 2000 (for the two measuring points of the sandy loam lysimeter)

Time period/site	a (cm d^{-1} mV^{-1})	b (cm d^{-1})	r^2
Days 30–140/S. Loam 1	0.0094	0.032	0.171[a]
Days 30–140/S. Loam 2	0.0064	−0.074	0.342[a]
Days 1–140/Clay Loam	1.93×10^{-4}	1.16×10^{-3}	0.470[a]
Rainfall 1 (days 91–101)/S. Loam 1	0.0077	−0.054	0.751[a]
Rainfall1 (days 92–101)/S. Loam 2	6×10^{-4}	0.031	0.0060

[a] 1% confidence level.

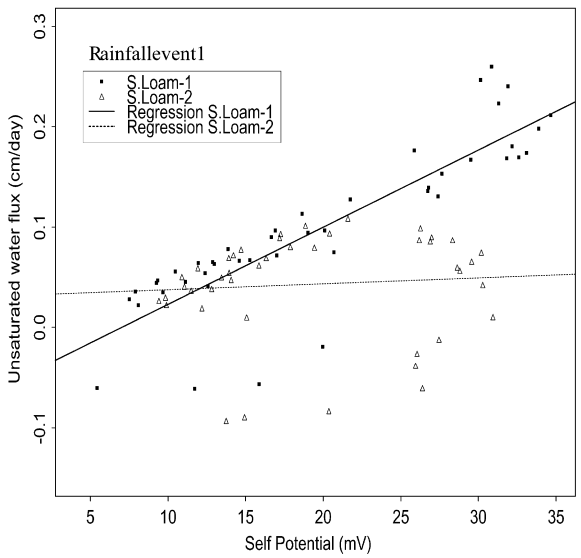

Fig. 7. Relationship between SP at 30 and 40 cm depth (i.e. $V_{40cm} - V_{30cm}$, where V is the electric potential at indicated depth) and the soil–water flux at 35 cm depth for the two measuring points (S. Loam 1 and S. Loam 2) in the sandy loam lysimeter for the first rainfall event of spring 2000 (23 mm). Regression lines Flux = aSP + b are also shown (see Table 1 also).

rewritten as:

$$\text{Flux} = \left(a\frac{\theta}{\theta_s} + b\right)\text{SP} + \left(c\frac{\theta}{\theta_s} + d\right) \quad (6)$$

where θ is the volumetric water content and θ_s is the volumetric water content at saturation. θ/θ_s is the water saturation.

At the scale of a rainfall event, Eq. (6) significantly improves the regression fits (see Table 2), as can be seen in Fig. 8A showing the soil–water fluxes estimated by linear regression (Eq. (6)) and measured for the first rainfall event. However, the fitted coefficients (a, b, c, d—Eq. (6)) vary between the different rainfall events, meaning that Eq. (6) is not stable with time. To increase its stability, Eq. (6) was fitted by splitting the infiltration and drainage phases of the different rainfall events. An example of the results of this fitting procedure is given in Fig. 8B and in Table 2 for the first rainfall event. A good fit of the fluxes corresponding to the different rainfall events can be obtained by applying this procedure. However, even in this case, Eq. (6) is not stable with time and the coefficients are both site and event-dependent.

The SP–unsaturated flux relationship can effectively be improved by taking into account the soil–electrode contact with the saturation variations. However, the instability of this relationship tends to show that other processes can induce a shift in the SP signal. One of these processes could be time variations of the pore water electrical conductivity (see Eq. (4)). On the studied site, where soils are calcareous, the soil–water electrical conductivity was rather buffered at 35 cm depth with a mean value of 500 ± 49 μS cm^{-1}. On the other hand, the pore water of the salted soil mud that was in contact with the electrodes showed a drastic variation of electrical conductivity (Fig. 9). This may have induced a variable 'electric' environment between the electrodes, as well as differences in the electric field sampled by the electrodes, and caused an additional SP drift with time.

4. Conclusion

The existence of a linear relationship between the

Table 2
Coefficients of the linear regression between SP (i.e. $V_{40cm} - V_{30cm}$, where V is the electric potential at indicated depth) and soil–water flux at 35 cm depth, taking into account a variable soil–SP electrode contact through water saturation, Eq. (6)). Data for the first rainfall event (23 mm) in spring 2000 and the two measuring points of the sandy loam lysimeter. Regression is calculated either by considering the total period of infiltration and drainage or by fitting independently the infiltration and drainage phases

Time period/site/process	a (cm d^{-1} mV^{-1})	b (cm d^{-1} mV^{-1})	c (cm d^{-1})	d (cm d^{-1})	r^2
Rainfall 1 (days 91–101)/S. Loam 1	−0.061	0.0394	2.194	−1.208	0.827
Rainfall1 (days 92–101)/S. Loam 2	0.0645	−0.0435	1.643	−0.812	0.898
Rainfall1 (days 91–93)/S. Loam 1/infiltration	0.0184	−0.0071	4.899	−2.51	0.997
Rainfall1 (days 93–101)/S. Loam 1/drainage	−0.0963	0.061	0.943	−0.562	0.934
Rainfall1 (days 92–96)/S. Loam 2/infiltration	0.0388	−0.0304	2.593	−1.335	0.958
Rainfall1 (days 96–101)/S. Loam 2/drainage	0.006	−0.0018	1.149	−0.638	0.917

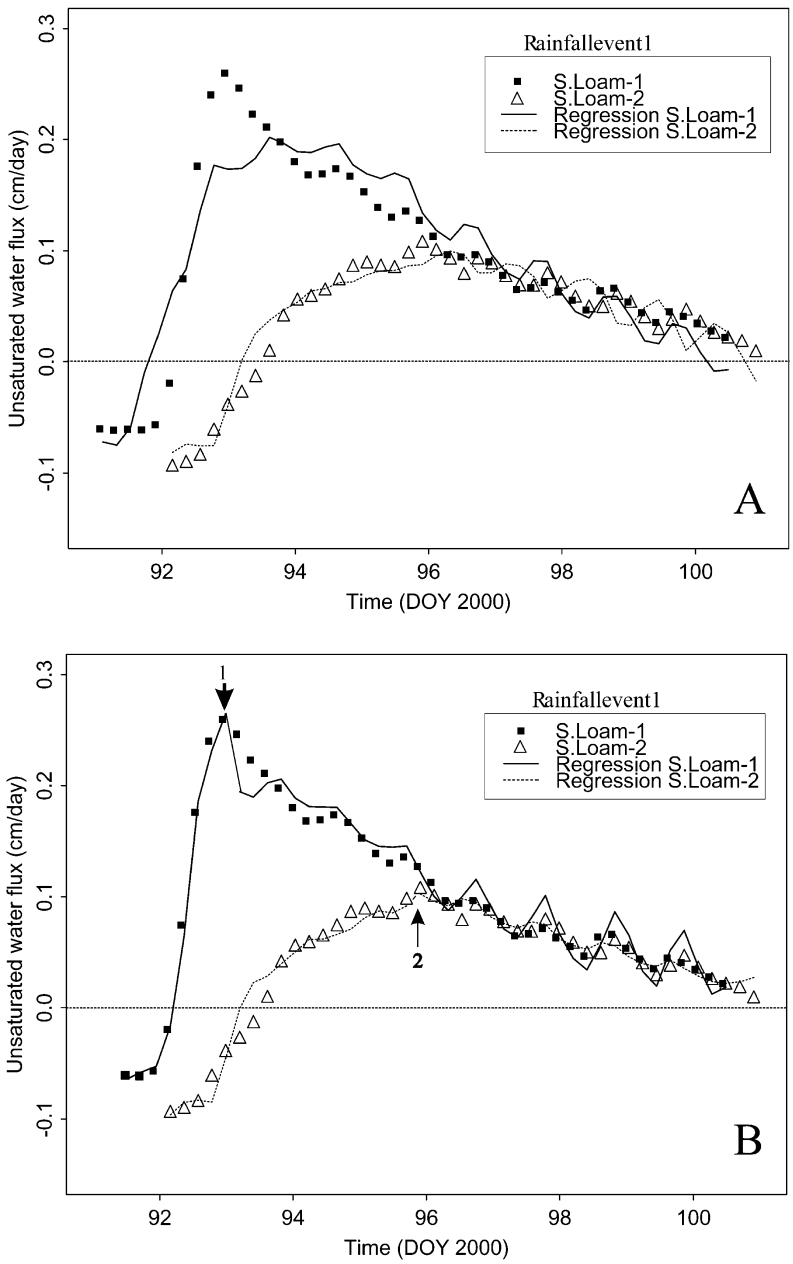

Fig. 8. (A) Comparison between the calculated soil–water fluxes and the field estimated water fluxes for the two measuring points (S. Loam 1 and S. Loam 2) in the sandy loam lysimeter. The flux–SP relationship Eq. (6) taking into account a variable soil–electrode contact through water saturation, is used to calculate flux. Data for the first rainfall event of spring 2000 (23 mm), see Table 2 also. (B) Same as A, but the flux–SP relationship (6) is fitted independently to the infiltration and drainage phases of the rainfall event (see Table 2 also). Arrows show the end of the infiltration phase and the beginning of drainage for the two measuring points.

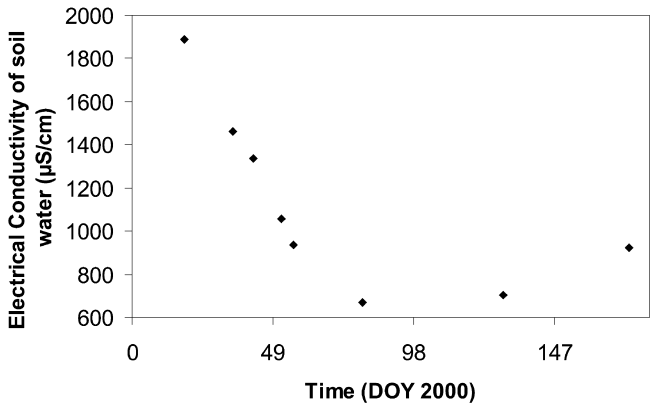

Fig. 9. Variation with time of the pore water electrical conductivity of the NaCl salted soil mud collected with suction cups installed similarly to the SP electrodes (sandy loam soil).

unsaturated water fluxes in soils and the SP could be very useful in research fields linked to soil physics. Thony et al. (1997) gave an experimental evidence of such a relationship. Estimation of water fluxes in soil is essential, but is difficult to obtain and highly variable in space and time. Indirect estimation of water fluxes by electrical measurements could lead to the design of an unsaturated fluxmeter that would be much more flexible and much easier to set-up than current measurements. The aim of this study was to investigate the existence and robustness of such a flux–SP relationship for different soil types and pedoclimatic conditions than in Thony et al. (1997) experiment.

Soil–water fluxes and SP were monitored in a long-term experiment involving two soil types, contrasting in hydraulic and electric properties, placed in lysimeters under the same meteorological conditions.

Measured time variations of SP are clearly linked to both rainfall events and evaporation. However, in the long-term, the quality of the linear relationship between the unsaturated water flux and SP ranged from a strong to a weak correlation. The slope of the flux–SP relationship seems to vary with the soil type and decreases with a more electrically conductive soil. Taking into account a varying soil–electrode contact, through water saturation (Eq. (6)), greatly improves the flux–SP relationship at the scale of a rainfall event, particularly when considering infiltration and drainage phases. Nevertheless, at the scale of a year, with alternated rainfalls and evaporation phases, the relationship (6) is not so robust (i.e. the coefficients of Eq. (6) vary between events). This variability could be attributed to variations in the electrical conductivity, not so much of the soil–water which is rather constant on the studied sites, but more of the salted mud that was added to the SP electrodes during their set-up. A variability of the flux–SP relationship is also observed between neighbouring data acquisition points in the same lysimeter, but this could be due to heterogeneity in the soil hydrodynamic characteristics. Estimation of this variability is currently undertaken.

This study points out methodological problems in measuring the SP in the shallow unsaturated zone, for long-term monitoring, in relation to water fluxes. The SP electrodes generally give accurate results in regular geophysical uses because of short-term measurements (e.g. mineral exploration) and/or burying at sufficient depths to avoid variations of saturation and temperature. A great amount of salted clay, in rather big holes, is also added. In these regular uses, SP variations linked to soil–water fluxes are most of the time considered as noise in the signal. In the case where the upper few meters of the soil and its hydrodynamics are of interest, very large variations of saturation, water potential, and temperature will occur throughout the season. Consequently, a design of electrodes maintaining electrical contact with varying conditions is essential. Important design parameters shape the electrode to avoid crack formation and the nature of the porous medium separating the electrolyte from soil, which should not desaturate in dry

conditions. Set-up conditions are also important, which should be as little disturbing as possible, and the effect of added salted mud should be much more specifically studied for this kind of SP application. The salted mud can lixiviate and its concentration can vary during periods of high drainage. This last point also stresses out the problem of agricultural fields where fertilizers are periodically added that may modify soil–water electrical conductivity.

However, with the present measurement devices, in the cases of slowly fluctuating conditions within a limited range, as it is often the case in deep soils beneath the root zone (where variations of temperature, saturation and chemistry of the soil solution are low), more stable flux–SP relationships with time could possibly be obtained. In this case, the use of SP data would be of great interest for examining/monitoring aquifer recharge, capillary rises or contaminant transfer.

Laboratory studies, with controlled temperature, water fluxes, and soil properties are needed to design electrical measurement devices better and also to get better insights into the unsaturated fluxes–SP relationship.

Acknowledgments

This study benefited from a grant INSU-CNRS 'Programme National de Recherche en Hydrologie (PNRH)' no PNRH-62-200—Research program 'Apport des méthodes géophysiques en hydrologie'. The authors thank Yves Dudal for kindly reviewing the language of the manuscript.

References

Adamson, A.W., 1976. Physical Chemistry of Surfaces, Wiley-Interscience, New York.

Ahmad, U., 1964. A laboratory study of streaming potentials. Geophys. Prospect. XII, 49–62.

Aubert, M., Dana, I., 1994. Interpretation of the self-potential radial profiles in vulcanology. Possibilities of the SP method for monitoring the actives vulcanoes. Bull. Soc. Geol. Fr. 165, 113–122.

Dukhin, S.S., Derjaguin, B.V., 1974. In: Matijevic, E., (Ed.), Surface and Colloid Science, vol. 7. Wiley, New York.

Gee, G.W., Ward, A.L., Kirkham, R.R., Ritter, J.C., 1999. A water-flux meter for unsaturated soils. Proceedings of the Annual Meeting ASA, CSSA, SSSA, 31 October–4 November, Salt Lake City, USA, 173.

Hashimoto, T., Tanaka, Y., 1995. A large self-potential anomaly on Unzen vulcano, Shimabara peninsula, Kyushu island, Japan. Geophys. Res. Lett. 22, 191–194.

Hillel, D., 1974. L'eau et le sol—Principes et processus physiques, Vander Editions, Louvain, Belgium.

Hunter, R.J., 1981. Zeta Potential in Colloid Science, Academic Press, London.

Ishido, T., 1989. Self-potential generation by subsurface water flow through electrokinetic coupling, Detection of subsurface flow phenomena, lecture notes in earth science, 27. Springer, New York, p. 121–131.

Ishido, T., Mizutani, H., 1981. Experimental and theoretical basis of electrokinetic phenomena in rock–water systems and its applications to geophysics. J. Geophys. Res. 86, 1763–1775.

Jensen, C.R., Svendsen, H., Andersen, M.N., Lösch, R., 1993. Use of the root contact concept, an empirical leaf conductance model and pressure volume curves in simulating crop water relations. Plant Soil 149, 1–26.

Jouniaux, L., Pozzi, J.P., 1995. Streaming potentials and permeability of saturated sandstones under triaxial stress. Consequences for electrotelluric anomalies prior to earthquakes. J. Geophys. Res. 100, 10197–10209.

Jouniaux, L., Bernard, M.L., Zamora, M., Pozzi, J.P., 2000. Streaming potential in volcanic rocks from Mount Pelée. J. Geophys. Res. 105 (B4), 8391–8401.

Lorne, B., Perrier, F., Avouac, J.P., 1999. Streaming potential measurements—2. Relationships between electrical and hydraulic flow patterns from rock samples during deformation. J. Geophys. Res. 104, 17879–17896.

Mitzutani, H., Ishido, T., Yokokura, T., Ohnishi, S., 1976. Electrokinetic phenomena associated with earthquakes. Geophys. Res. Lett. 3, 365–368.

Morat, P., Le Mouël, J.L., 1992. Signaux électriques engendrés par des variations de contrainte dans des roches poreuses non saturées. C. R. Acad. Sci. Paris, Serie II 315, 955–963.

Nourbehecht, B., 1963. Irreversible thermodynamic effects in inhomogneous media and their applications in certain geoelectric problems. PhD Thesis, Massachusetts Institute of Technology, Cambridge.

Overbeek, J.Th.G., 1952. Electrochemistry of the double layer. In: Kruyt, H.R., (Ed.), Colloid Science, Irreversible Systems, vol. 1. Elsevier, New York, pp. 115–193.

Perrier, F., Petiau, G., Clerc, G., Bogorodsky, V., Erkul, E., Jouniaux, L., Lesmes, D., Macnae, J., Meunier, J.M., Morgan, D., Nascimento, D., Oettinger, G., Schwarz, G., Toh, H., Valliant, M.J., Vozoff, K., Yaziciçakin, A., 1997. A one year systematic study of electrodes for long period measurements of the electric field in geophysical environments. J. Geomagn. Geoelectr. 49, 1677–1696.

Perrier, F., Trique, M., Lorne, B., Avouac, J.P., Hautot, S., Tarits, P., 1998. Electrical variations associated with yearly lake level variations. Geophys. Res. Lett. 25, 1955–1958.

Perrier, F., Trique, M., Aupiais, J., Gautam, U., Shrestha, P., 1999. Electric potential variations associated with periodic spring

discharge in western Nepal. CR Acad. Sci. Paris, Serie II 328, 73–79.

Petiau, G., 2000. Second generation of Lead–Lead Chloride electrodes for geophysical applications. Pure Appl. Geophys. 157, 357–382.

Pride, S.R., 1994. Governing equations for the coupled electromagnetics and acoustics of porous media. Phys. Rev. B: Condens. Matter 50, 15678–15696.

Revil, A., Pezard, P.A., Glover, P.W., 1999A. Streaming potential in porous media—1. Theory of the zeta potential. J. Geophys. Res. 104 (B9), 20021–20031.

Revil, A., Schwaeger, H., Cathles, L.M., Manhardt, P.D., 1999b. Streaming potential in porous media—2. Theory and application to geothermal systems. J. Geophys. Res. 104 (B9), 20033–20048.

Tamari, S., Bruckler, L., Halbertsma, J., Chadoeuf, J., 1993. A simple method for determining soil hydraulic properties in the laboratory. Soil Sci. Soc. Am. J. 57, 642–651.

Thony, J.L., Morat, P., Vachaud, G., Le Mouël, J.L., 1997. Field characterization of the relationship between electrical potential gradients and soil water flux. CR Acad. Sci. Paris, Earth Planetary Sci. 325, 317–321.

Vachaud, G., Dancette, C., Sonko, M., Thony, J.L., 1978. Méthodes de caractérisation hydrodynamique in situ d'un sol non saturé. Application à deux types de sols du Sénégal en vue de la détermination des termes du bilan hydrique. Ann. Agro. 29, 1–36.